Available online at www.sciencedirect.com

ScienceDirect

Russian Geology and Geophysics 58 (2017) 650–658

RUSSIAN GEOLOGY AND GEOPHYSICS

www.elsevier.com/locate/rgg

Inversion of magnetotelluric data in fault zones of Gorny Altai based on a three-dimensional model

V.V. Plotkin *, E.V. Pospeeva, D.I. Gubin

A.A. Trofimuk Institute of Petroleum Geology and Geophysics, Siberian Branch of the Russian Academy of Sciences, pr. Akademika Koptyuga 3, Novosibirsk, 630090, Russia

Received 27 October 2015; accepted 16 March 2016

Abstract

Results of magnetotelluric sounding (MTS) in Gornyi Altai are interpreted on the basis of a numerical model of MTS curve distortions in a 3D earth. The distortions are modeled using the Trefftz method permitting the application of models of different degrees of similarity to the test medium (depending on available computational resources). The main advantages of this approach are demonstrated. There is no need to choose between different MTS curves (transverse and longitudinal, minimum and maximum, undistorted and distorted). Procedures of normalizing these curves become unnecessary. All recorded curves are fully used as input data for their inversion. Optimization of the model of the medium taking into account the distortions of MTS curves caused by surface and depth inhomogeneities improves the reliability of geoelectric sections.

Keywords: magnetotelluric sounding; electrical conductivity; distortions and normalization of MTS curves; surface and depth inhomogeneities; geoelectric section; recent faults; Cenozoic activation

Introduction

Identification and study of active fault zones helps to solve problems of modern geodynamics and is an essential element of seismic zonation and seismic hazard evaluation. Faults as dominant geological structures of different scales are assigned a key role in the structural control of fluid permeability and recent phenomena in the upper part of the Earth's lithosphere. In seismology, the relationship between earthquakes and faults has long been established: the development of fault zones is accompanied by seismicity and is associated with deformations of the crust and lithosphere, which contribute to tectonic movements (Sherman and Seminsky, 2010) and are identified in the surface relief. Faults with a long geological history, latent faults of the basement, lineaments, and their intersection nodes are seismically active (Kalinina, 2005; Kalyagin and Abramov, 2003). Deep faults are in fact through channels penetrating into the lower crust and upper mantle, as well as alkaline ultrabasic and carbonatite magma fluid columns reaching hypabyssal depths and even the Earth's surface (Kadik, 2006). Major earthquakes are almost always confined to active faults. This is confirmed by experimental data showing that a sudden rise of fluids in fault zones initiates an earthquake (Aptikaev, 1995).

One method for studying active faults is magnetotelluric sounding (MTS). Deep fluid-saturated faults form conductive channels which intersect the high-ohmic lithosphere to provide vertical redistribution of excess currents and are fixed in the magnetotelluric field in the form of subvertical conductive geoelectric inhomogeneities (Batalev et al., 2013; Berdichevsky et al., 1999; Epov et al., 2011; Maercklin et al., 2005; Nevedrova et al., 2014; Pospeeva et al., 2014; Unsworth and Bedrosian, 2004; Unsworth et al., 1999). The identification of earthquake patterns in relation to geological-tectonic features and neotectonics has motivated magnetotelluric studies in Gornyi Altai, which is one of the most dangerous seismic regions in Russia. An important aspect of these studies is to choose a valid methodological approach to the interpretation and analysis of the data obtained.

The complex geoelectric structure of the medium near faults complicates the analysis of the behavior of magnetotelluric curves. In particular, one has to use various coefficients to check the two-dimensionality conditions of geoelectric structures, to choose undistorted curves or perform their normalization (Moroz and Moroz, 2012; Nevedrova et al., 2011).

* Corresponding author.
E-mail address: PlotkinVV@ipgg.sbras.ru (V.V. Plotkin)

1068-7971/$ - see front matter
http://dx.doi.org/10.1016/j.rgg.2017.04.006

At sounding stations near a fault, the maximum and minimum curves usually differ in resistivity, and additional minima and maxima appear, depending on the sounding period. However, this behavior of magnetotelluric curves is quite typical of distortions that occur in the presence of surface and subsurface inhomogeneities of electrical conductivity (Plotkin and Gubin, 2015).

By distortions are usually meant differences between recorded magnetotelluric curves and the local curve corresponding to a horizontally layered section with the electrical conductivity dependent on the depth under the sounding station. Lateral changes in this dependence lead to various distortions of the electromagnetic field and additional contributions to the impedance tensor. The response of the medium becomes nonlocal, but due to the diffusion nature of field propagation in a conductive medium, the distortions of the curves are determined by the confined volume of the medium near the sounding station (Plotkin, 2012). Neglect of the possible distortions of the curves may lead to misinterpretation of MTS data on the deep structure of faults. In particular, distortions caused by near-surface inhomogeneities may be interpreted as a deep conductive layer.

On the other hand, modeling of these distortions in the interpretation of MTS data using all available magnetotelluric curves (longitudinal, transverse, phase) for several stations can narrow the equivalence regions of the inverse problem solutions. In (Plotkin and Gubin, 2015), distortions are modeled using the Trefftz method (Egorov, 2011), a feature of which is that the software code allows using models of varying degrees of similarity to the test medium. Changing the detail of representation of the medium, it is possible to find a compromise between the achievable quality of experimental data interpretation and the computational cost of processing. At the same time, the similarity of the inverse problem solutions in these cases confirms their accuracy and a decrease in the equivalence region.

It should be noted that at high latitudes or in the equatorial zone where there are powerful ionosphere currents—electrojets (Zhdanov, 1986), the approximation of a primary source by a vertically incident plane wave ceases to hold. The inhomogeneous structure of the source should be taken into account. The difficulties that arise can be overcome by using synchronous areal sounding. In this case, there is no need to know the origin of spatial harmonics of the fields (from the source or from the medium) on the Earth's surface, and the magnetic or electrical field component distributions recorded on the Earth's surface can be used as the upper boundary conditions (UBC). The inverse problem solution can be found by matching these distributions on the surface to each other (Plotkin, 2012) and without using and calculating MTS curves.

In the mid-latitudes, there is no need to use synchronous probing because in the far-field zone of the primary source, it is valid to assume that the medium is excited by a vertically incident plane wave. This implies that lateral changes of the field on the Earth's surface are due only to the inhomogeneity of the medium. Therefore, it is possible to use UBC (Plotkin and Gubin, 2015) which take into account that the spatial harmonics of the field excited in the medium are attenuated deep in the atmosphere. This case is the subject of the present paper.

Data used and inversion procedure

To analyze the possibilities and implementation of this approach, we used the results of magnetotelluric profiling performed within the Ulagan Plateau located in the East-Altai facies zone. This zone is between the Gorny Altai and West Sayan folded systems and is often included in the latter (Kuznetsov, 1963). In the southwest, it is bounded by the Kurai–Teletsk deep fault, whose eastern part breaks into a series of feathering faults. The upper structural level of the East-Altai structural zone is formed by basins composed of terrigenous sedimentary rocks, in particular, Devonian clastic sediments. Metamorphic ridges, previously considered as basement rocks, are currently interpreted as Lower–Middle Paleozoic metamorphosed rocks with a complex laminated-overlapped tectonic structure (Novikov, 2004). The profile in question is located in the interfluve between Bashkaus and Yoldu (Fig. 1*a*), within which the upper structural level rocks are primarily sandstones and siltstones of the Gorny Altai Formation ($Є_3$–O_{1gr1}) and metamorphic schists of the Lower Proterozoic Terekta Formation ($PR_{tr?}$). These formations are characterized by high electrical resistivity, which varies from 2000–2500 Ohm·m in the southwestern part of the profile to 7000–10,000 Ohm·m in the northeast. In the middle part of the crustal section, there is a conductive layer with the upper edge at a depth of 10–12 km and a resistivity of less than 50 Ohm·m. The layer is complicated by a series of subvertical conductive inhomogeneities within which the resistivity is about 5 Ohm·m. The inhomogeneities are spatially associated with a system of recent northwest-trending faults reconstructed from the results of geomorphological studies (Novikov, 2001). According to these studies, the faults, active in the Cenozoic, form a block system with significant (hundreds and thousands of meters) displacement amplitudes during the Late Cenozoic time and form the basis of the modern orographic structure (large relief forms such as ranges and intermontane basins).

In Fig. 1*a*, faults are shown by wide black and gray stripes. MTS stations 7–18 of the profile are located along one of these faults (black). The profile is intersected by two other faults (gray) in the vicinity of stations 9 and 13.

In the simulation using the Trefftz method, the computational domain of the inhomogeneous medium is represented by a set of several finite elements in the form of parallelepipeds, in which the medium is homogeneous. As an example, Fig. 1*b* shows a diagram of the polygon and the projections of the parallelepipeds onto the surface. The coordinate system is placed at the location of the base station 13 (the *OX* and *OY* axes are arranged in a horizontal plane, and the OX axis is directed along an azimuth of 45° with respect to the geographic north, i.e., along the selected profile, the *OZ* axis is directed downward, and the Earth's surface $z = 0$). In Fig. 2, the apparent resistivity curves at the stations of the profile are

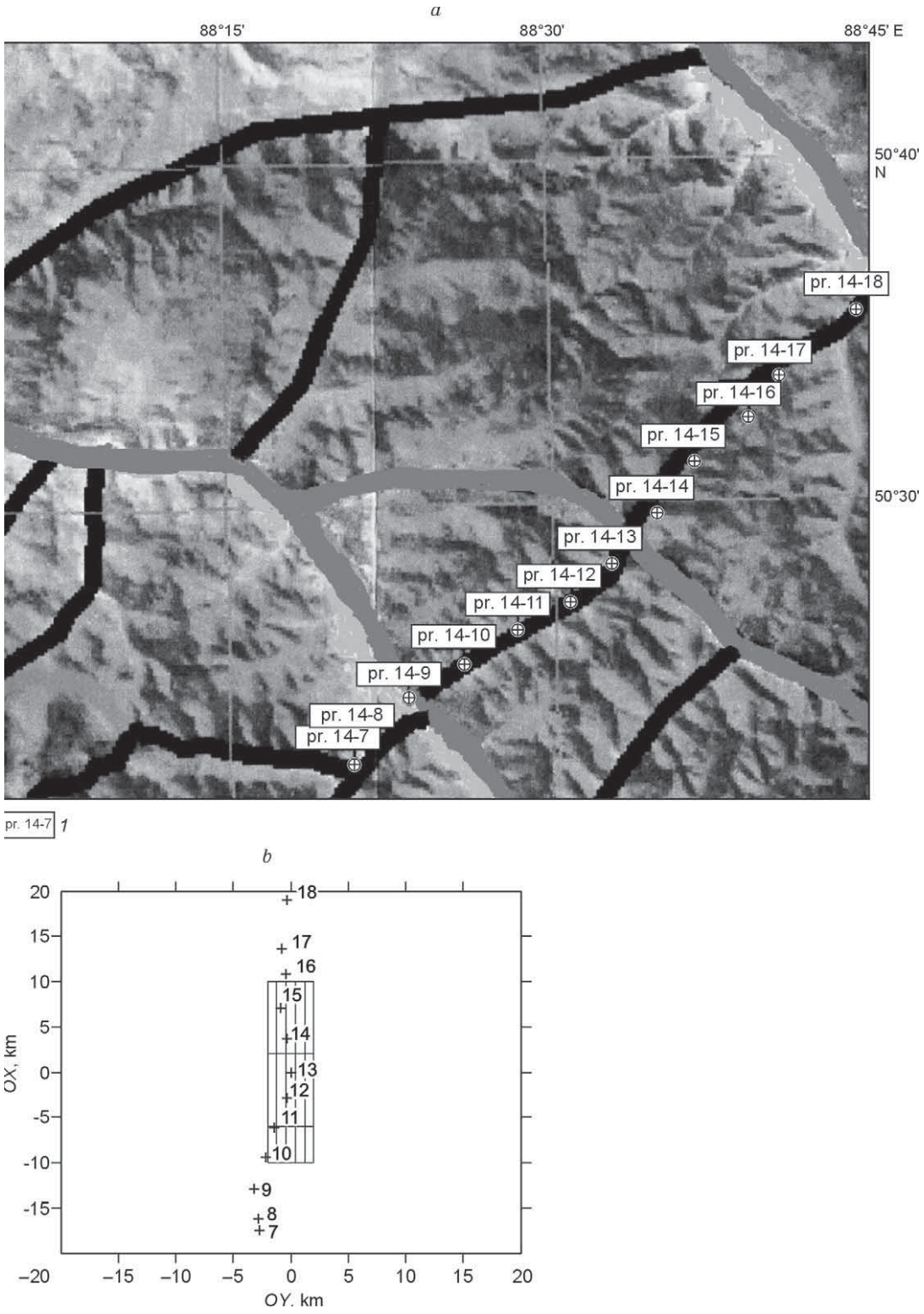

Fig. 1. Geological map of the study area of Altai. *a,* Faults are shown by wide stripes; *1*, profile 14–MTS station number; *b*, projection of the computational domain onto the surface of the polygon; stations are shown by crosses with an indication of their numbers.

given for this coordinate system. As can be seen, at stations 9 and 13, the distortions of the curves are most apparent, and the divergence of the longitudinal and transverse curves reaches two orders of magnitude.

In the simulation, we used a computational domain with a partition of the polygon into three to seven parallelepipeds along the horizontal axis and with up to four inhomogeneous layers along the depth. This was sufficient to obtain all the

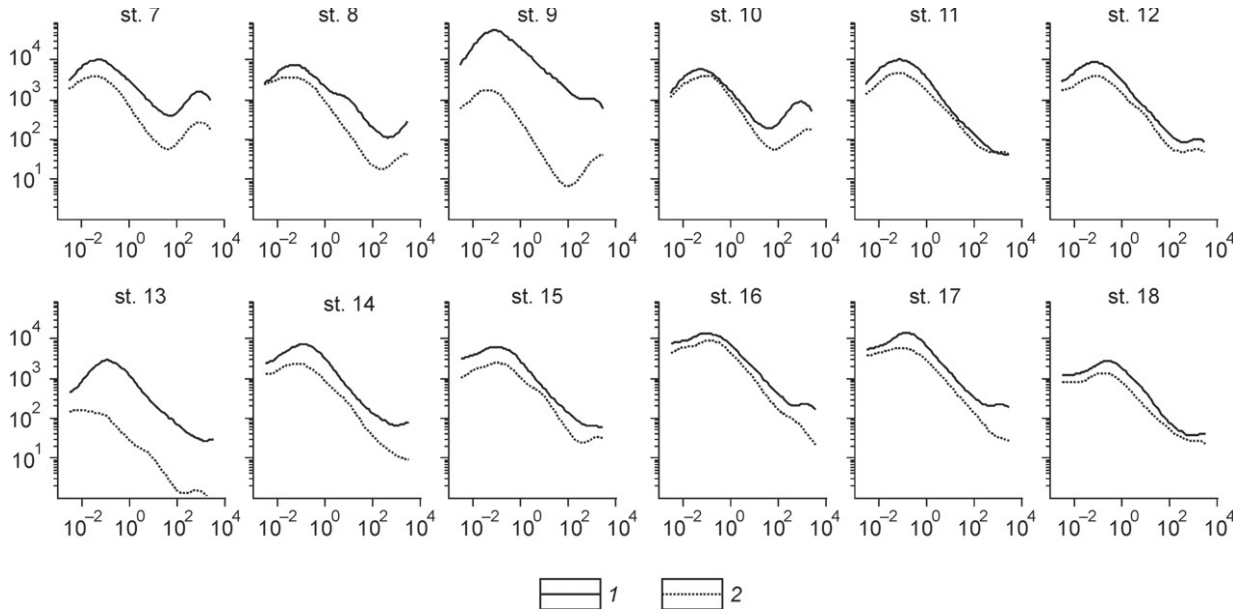

Fig. 2. Apparent resistivity curves at MTS stations relative to the profile. *1*, longitudinal, *2,* transverse; the station numbers are given above each graph; the time period is plotted on the abscissa (a), the apparent resistivity is plotted on the ordinate (Ohm·m).

characteristic features in the behavior of magnetotelluric curves at the stations.

The optimization of the conductivity in the parallelepipeds was carried out in stages to expedite the work. In the modeling, we first used a smaller volume of the medium (with a partition into three finite elements along the horizontal axes) and only the data of station 13 at the center of the polygon. Then, the analyzed volume of the medium was increased to seven parallelepipeds along the *OX* and *OY* axes and the data of several stations were invoked.

The dimensions of the parallelepipeds along the horizontal axes were varied: h_x (along the *OX* axis) from 1 to 5 km, and h_y (along the *OY* axis) from 0.1 to 1.5 km. Selecting the aspect ratio of the parallelepipeds was essential for modeling magnetotelluric curves at the data acquisition stations and optimizing the earth model. In particular, the sides of the parallelepipeds along the profile far exceed the sides transverse to it (Fig. 1*b*). This is due to the fact that with equal horizontal dimensions of the parallelepipeds, it was not possible to obtain all features of the behavior of the curves at the stations. This may be due to the small offset between the stations and the profile line (Fig. 1*b*). This arrangement of the observation stations does not allow obtaining sufficient areal data in directions transverse to the profile to determine the structure of the medium in these directions. The position of the projections of the parallelepipeds onto the surface of the polygon relative to the profile stations was also of significance. Consequently, the use of a rough earth model in each case requires an adequate observation system that takes into account the complex geoelectric structure—the intersections of faults in the Earth's crust, etc.

Therefore, in the optimization of the earth model with the available profile data, the desired parameters included not only the electrical conductivities in the parallelepipeds, but also their variable horizontal dimensions h_x and h_y, and the thicknesses of the inhomogeneous layers. Note that in the calculations, the stations have fixed coordinate, in particular, the base (central station) always has coordinates (0, 0). The curves for each parallelepiped that contains a station are calculated above the point at the center of the parallelepiped. Therefore, the computational point coincides with the position only for the base station, whereas for the remaining stations, the computational points may be shifted relative to the position of these stations ~h_x and h_y. Therefore, the geometry of the obtained sections is known only with this accuracy. In practice, the inversion results for different initial horizontal dimensions of parallelepipeds manifest themselves as a contraction or extension of the obtained sections along the horizontal axes by distances ~h_x and h_y. This is a consequence of the fundamental ambiguity of interpretation of experimental data that are not fully adequate to the earth structure, resulting in the equivalence of the obtained models (Tabarovskii and Epov, 2006). A denser observation network is needed to narrow the model-driven equivalence domain.

The degree of fit of the earth model to the available experimental data can be judged by the minimum of the objective functional which defines the residual between the calculated and measured MTS curves:

$$\Phi = \frac{1}{2KJ} \sum_{k=1}^{K} \sum_{j=1}^{J} \left(\left| \frac{\rho_{xy}^{t} - \rho_{xy}^{\exp}}{\rho_{xy}^{\exp}} \right|^2 + \left| \frac{\rho_{yx}^{t} - \rho_{yx}^{\exp}}{\rho_{yx}^{\exp}} \right|^2 \right)_{k,j}, \quad (1)$$

where ρ_{xy}^{t}, $\rho_{xy}^{\exp}$, ρ_{yx}^{t}, $\rho_{yx}^{\exp}$ are the apparent resistivities (the subscripts *xy* and *yx* denote different field polarizations, and the superscripts *t* and exp refer to the simulated and experimental apparent resistivities, respectively) obtained at different

stations (summation over k) and for different periods (summation over j). Similarly, terms that take into account the differences between the experimental and theoretical phase impedances are also written in parentheses in functional (1). The reliability of inversion results can be evaluated by comparing the results with and without consideration of phase residuals as well as the residuals for the data on the vertical component of geomagnetic variations. Note that functional (1) does not take into account the experimental measurement errors, by which, generally speaking, the corresponding denominators of all the terms in (1) should be replaced. This is clear from the fact that minimizing the deviations between theoretical and experimental MTS curves below the error level hardly makes sense. Because it is more convenient to compare the differences between the model and experimental curves in percent, we use functional (1), assuming that the measurement accuracy of the experimental values is high and their errors are small compared with the errors of inverse problem solutions. Thus, for comparison of the results, the minima of (1) obtained by inversions are used as the average deviations between the measured and model MTS curves, expressed as a percentage for one measurement. The model was optimized using the Nelder–Mead method until the minimum of the functional reached a predetermined value or until its changes became smaller than the threshold value.

In the data inversion, the earth model was parameterized in a form that takes into account the a priori known maximum and minimum values of the desired quantities; for example, for the electrical conductivities:

$$\sigma = \exp(\sigma_0 + \sigma_1 \operatorname{th}(x)),\ \sigma_0 = \ln(\sqrt{\sigma_{\max}\sigma_{\min}}),$$
$$\sigma_1 = \ln(\sqrt{\sigma_{\max}/\sigma_{\min}}), \quad (2)$$

where $-\infty < x < \infty$ and $\sigma_{\max}$ and $\sigma_{\min}$ are the maximum and minimum electrical conductivities (in the parallelepipeds and underlying layers), respectively. Expressions similar to (2) were also used for the other parameters—the horizontal dimensions of the parallelepipeds and the thickness of the inhomogeneous layers. Instead of (2) we also used simpler expression of the form $\sigma = \exp(x)$, together with the boundedness condition for the ranges of the corresponding quantities. Experience has shown that the optimization of the earth model in this case was carried out with less iterations.

Inversion results and discussion

We performed several optimizations of the earth model, which differed in the starting electrical conductivities in the parallelepipeds, their original horizontal dimensions, and the number of inhomogeneous layers in depth. As an example, the results of one of the optimization runs are presented in Fig. 3, which shows the agreement between the model and experimental apparent resistivity curves at the stations involved (Fig. 3*a*). The final geoelectric model of the earth is represented by a three-dimensional volume distribution of resistivity on a logarithmic scale, and the observation stations are marked by crosses (Fig. 3*b*). As the starting model we used a two-dimensional geoelectric model with the structure extended along the *OY* axis. It is shown in Fig. 4*a*.

Practice has shown that the smaller the dimensions of the parallelepipeds in the Trefftz method, the lower the obtained minima in (1) (reducing the dimensions of the parallelepipeds with a simultaneous increase in their number requires considerable computational resources and is difficult in practice). Consequently, using parallelepipeds of smaller dimensions, we can consistently obtain models that more accurately reflect the structural features of the real earth.

Figures 4 and 5 show several types of 3D sections of distributions of the logarithms of the resistivity obtained by minimizing the objective functional Φ. All of them were obtained for different initial horizontal dimensions of the parallelepipeds h_x and h_y, with the number of parallelepipeds on the horizontal axes equal to 5 (except in Fig. 4*c*, where it is equal to 7).

The depth resistivity distributions in the vertical sections (with different dimensions h_x and h_y) through the base station 13 along the investigated profile (along the *OX* axis) are shown on the same scale along the coordinate axes in Fig. 4*b, d, f*. Similar distributions obtained from the data of the same stations for different dimensions of the polygon are shown in Fig. 4*c, e* (for the same dimensions of parallelepipeds, but with a partition of the computational domain along the horizontal axes into 7 and 5 parallelepipeds, respectively). Comparison of Figs. 4*c* and 4*e* characterizes the influence of the boundary conditions on the results with increasing the dimensions of the polygon. It can be seen that increasing the dimensions of the polygon affects the sections only within the error of the inversion problem solution.

Resistivity maps on the Earth's surface are given in Fig. 5 (left). The depth resistivity distributions in the vertical sections transverse to the test profile (along the *OY* axis) and passing through the base station 13 are shown in Fig. 5 (right). Recall that starting models (Fig. 4*a*) in the two-dimensional approximation is adopted for the case of no dependence along the *OY* axis. As can be seen from the depth sections transverse to the profile (Fig. 5, right), the conditions of the two-dimensional approximation are satisfied only locally in some intervals on the *OY* axis. This locality of the two-dimensional approximation of geoelectric sections is characteristic of intermittent manifestations of the deep fault on the Earth's surface according to MTS data. Probably, not all areas of the fault can be seen from these data.

The results of inversion with reduced original horizontal dimensions of parallelepipeds appear in Figs. 4 and 5 as contractions of the obtained sections along the horizontal coordinate axes. As already mentioned, the geometry of the obtained sections is only known with accuracy ~h_x and h_y. Comparison of the sections (Figs. 4 and 5) with close minima of the functionals presented on the same scale on the coordinate axes, but obtained with different initial dimensions of parallelepipeds gives an idea of the equivalence domains of the inverse problem solutions.

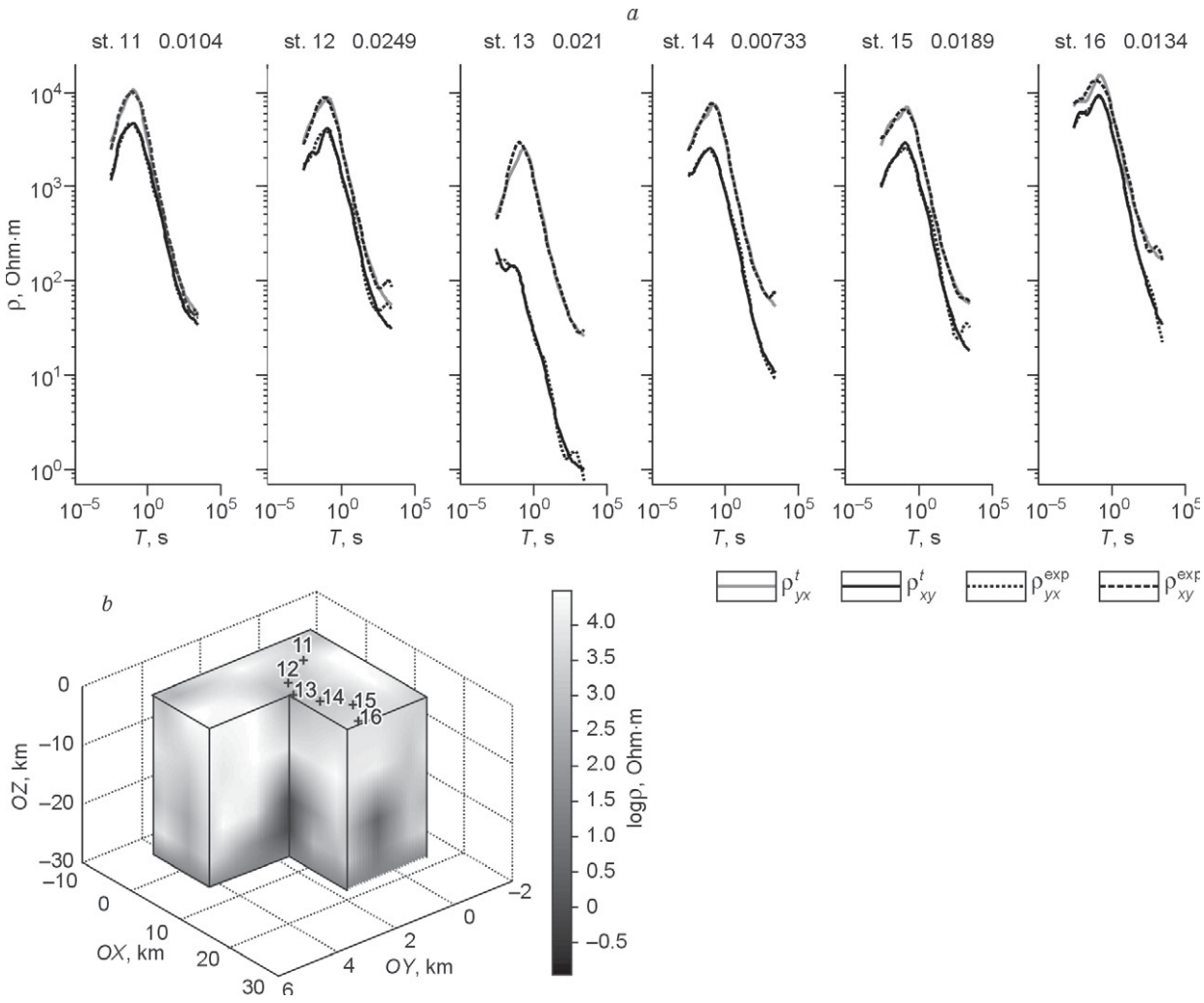

Fig. 3. Example of the result of minimization of the objective functional Φ with the obtained minimum $\Phi_{min} = 0.0152$. *a*, Apparent resistivity curves at MTS stations, the numbers above the plots are the average differences between the curves at the specified station; *b*, 3D geoelectric section.

As can be seen, increasingly smaller structural features of the real earth are reproduced as the dimensions of parallelepipeds are reduced. In particular, in Figs. 4 and 5, one can see that near station 13 (isolines on the Earth's surface and vertical sections), there is the region of intersection of two differently trending faults (along the profile and transverse to it) (Fig. 1*a*), which is responsible for the observed distortions of MTS curves at this station. We can therefore speak of a refinement of the obtained models. It is clear that excessive reduction in the original dimensions of parallelepipeds is limited by the density of the system of observation stations, in particular, the distance between them. The spatial field harmonics for which the distances between stations are larger more than half the wavelength will be perceived in data processing with the well-known aliasing effect (Kotel'nikov theorem) taken into account. Thus, the uncontrolled reduction in the dimensions of parallelepipeds to less than half the minimum distances between the stations is accompanied by the appearance of additional equivalent solutions of the inverse problem.

Conclusions

An important advantage of this approach is that it is suitable for solving inverse problems in the presence of significant distortions of MTS curves even in the case of a 3D earth. There is no need to analyze the standard coefficients of validity of the 2D approximation and to choose between different MTS curves (transverse and longitudinal, minimal and maximal, undistorted and distorted). Normalization of these curves becomes unnecessary. All recorded curves can be fully used as input data for the inversion procedure. Comprehensive consideration of MTS curve distortions, of course, increases the reliability of geoelectric sections.

This approach provides a real compromise between the accuracy of the inverse MTS problem solution and its computational cost. Coarser representations of electrical conductivity distributions in the earth can be obtained at lower cost in shorter time and, more importantly, with controlled accuracy.

The results of test applications of this method suggest a narrowing of the equivalence domains of the solutions ob-

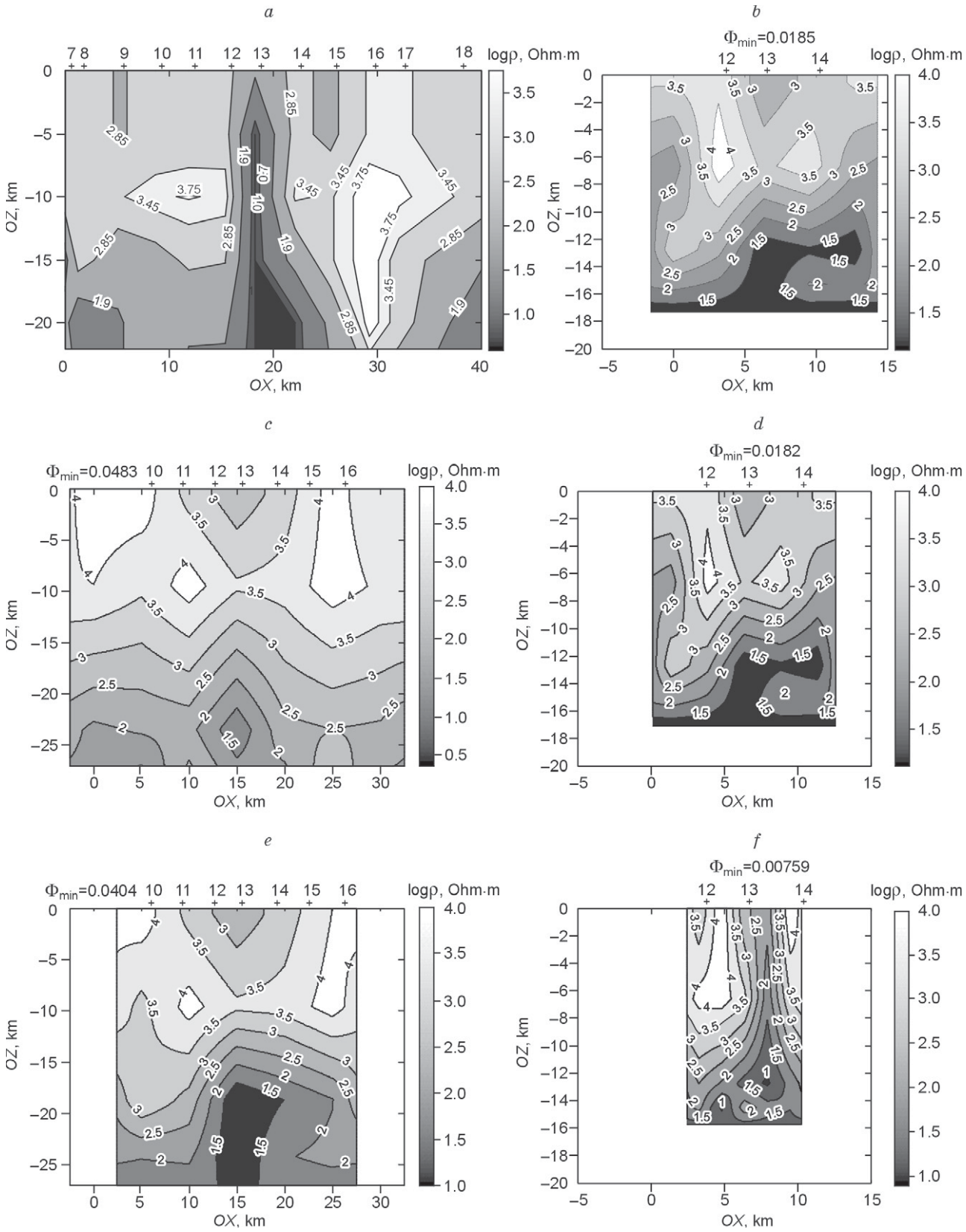

Fig. 4. Comparison of several results of minimization of the objective functional Φ. *a*, 2D depth section, the starting model; *b–f,* versions of 3D depth sections. All depth sections are given for the vertical section passing along the investigated profile through base station 13, the numbers above the plots indicate the obtained minima of the functional Φ.

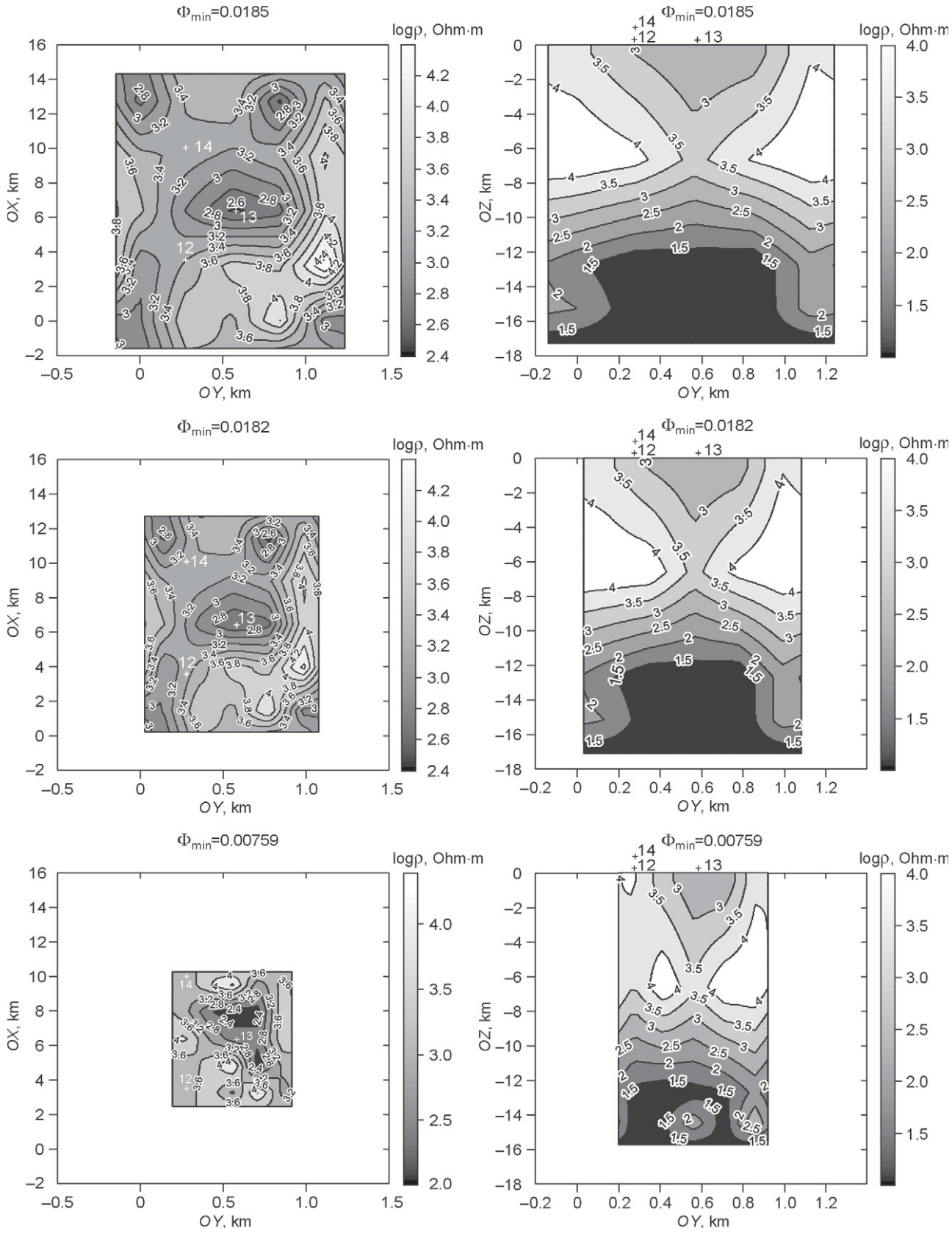

Fig. 5. Comparison of several results of minimization of the objective functional Φ. On the left are the distributions of the logarithms of the resistivity on the Earth's surface; on the right are depth sections transverse to the test profile, the numbers above the plots indicate the obtained minima of the functional Φ.

tained. This can be explained by an increase in the amount of data used as input for the inversion procedure, and from a physical point of view, by consideration of the total adjacent volume of three-dimensional earth around the sounding stations. It should, however, be emphasized that the model-driven equivalence of solutions arises if the chosen system of observation stations does not match the complexity of the structure of the medium.

From a practical point of view, these results allow a significant improvement in the reliability of data interpretation and hence the reliability of their geological explanation. In particular, the exact identification of active faults can improve the reliability of seismic zoning and seismic hazard assessment of the Gorny Altai region.

We thank V.V. Potapov for his great contribution to the experimental field work and reviewers—E. Yu. Antonov and the anonymous reviewer—for interest in the work and useful discussions.

References

Aptikaev, S.F., 1995. Structure of a Microscale Seismic Field: Abstracts of Candidate's Dissertation in Phys.-Mat. Sci. Moscow.

Batalev, V.Yu., Bataleva, E.V., Matyukov, V.E., Rybin, A.K., 2013. Deep structure of the western part of the Talas–Fergana fault from magnetotelluric data. Litosfera, No. 4, 136–145.

Berdichevsky, M.N., Van'yan, L.P., Koshurnikov, A.V., 1999. Magnetotelluric sounding in the Baikal rift zone. Fizika Zemli, No. 10, 3–25.

Epov, M.I., Nevedrova, N.N., Pospeeva, E.V., Sanchaa, A.M., Potapov, V.V., 2011. Geoelectric structure of the Earth's crust in the Chuya Basin of Gorny Altai based on an integrated interpretation of electromagnetic data with a controlled and natural source (MT, TEM), in: Dynamics of Physical Fields of the Earth [in Russian]. Svetoch Plyus, Moscow, pp. 31–53.

Egorov, I.V., 2011. Trefftz method for the solution of three-dimensional forward and inverse problems of geoelectrics. Fizika Zemli 47 (2), 15–26.

Kadik, A.A., 2006. Fluids as a reflection of the redox regime in the mantle: implications for the geophysical properties of deep material, in: Fluids and Geodynamics [in Russian]. Nauka, Moscow.

Kalinina, L.Yu., 2005. The Role of Faults and Deep Structure in the Spatial Control of Earthquakes in the Northeast of Russia. Abstracts of Dissertation in Geol.-Mineral. Sci. Magadan.

Kalyagin, A.N., Abramov, V.A., 2003. Fundamentals of Trans-Structural Geology [in Russian]. Dal'nauka, Vladivostok.

Kuznetsov, V.A., 1963. Tectonic zoning and the main features of endogenous metallogeny of Gorny Altai, in: Geology and Metallogeny of Gorny Altai [in Russian]. Novosibirsk, pp. 7–68.

Maercklin, N., Bedrosian P.A., Haberland C., Ritter O., Ryberg T., Weber M., and Weckmann, U., 2005. Characterizing a large shear-zone with seismic and magnetotelluric methods: The case of the Dead Sea Transform. Geophys. Res. Lett. 32, L15303, doi:10.1029/2005GL022724.

Moroz, Yu. F., Moroz, T.A., 2012. Anomalies in the electric field and electric conductivity of the Earth's crust in relation to the Kultuk earthquake on Lake Baikal. Fizika Zemli 48 (5), 64–76.

Nevedrova, N.N., Pospeeva, E.V., Sanchaa, A.M., 2011. Interpretation of complex electromagnetic data in seismically active regions: case study of the Chuya depression, Mountain Altai. Fizika Zemli 47 (1), 63–75.

Nevedrova, N.N., Deev, E.V., Sanchaa, A.M., 2014. Deep structure and margins of the Kurai basin (Gorny Altai), from controlled-source resistivity data. Russian Geology and Geophysics (Geologiya i Geofizika) 55 (1), (98–107) 119–132.

Novikov, I.S., 2001. Cenozoic strike-slip tectonics of Altai. Geologiya i Geofizika (Russian Geology and Geophysics) 42 (9), 1377–1388 (1311–1321).

Novikov, I.S., 2004. Morphotectonics of Altai [in Russian]. Izd. SO RAN, Filial Geo, Novosibirsk.

Plotkin, V.V., 2012. Medium and field inhomogeneity: zone of influence during magnetotelluric sounding. Russian Geology and Geophysics (Geologiya i Geofizika) 53 (1) 108–115 (140–149).

Plotkin, V.V., Gubin, D.I., 2015. Accounting for near-surface inhomogeneities over a horizontally layered section in magnetotelluric sounding. Russian Geology and Geophysics (Geologiya i Geofizika) 56 (7), 1083–1090 (1381–1390).

Pospeeva, E.V., Vitte, L.V., Potapov, V.V., Sakharova, M.A., 2014. Magnetotelluric studies in areas of recent tectonics and seismic activity: case study of Gorny Altai. Geofizika, No. 4, 8–16.

Sherman, S.I., Seminsky, K.Zh., 2010. Tectonophysical reserach at the Institute of the Earth's Crust: major achievements and actual problems. Geodinamika i Tektonofizika 1 (1), 4–15.

Tabarovskii, L.A., Epov, M.I., 2006. Estimating the resolution of electromagnetic methods. Russian Geology and Geophysics (Geologiya i Geofizika) 47 (5), 563–573 (568–578).

Unsworth, M., Bedrosian, P., 2004. On the geoelectric structure of major strike-slip faults and shear zones. Earth Planets Space 56, 1177–1184.

Unsworth, M.J., Egbert, G.D., Booker, J.R. 1999. High resolution electromagnetic imaging of the San Andreas Fault in Central California. J. Geophys. Res. 104, 1131–1150.

Zhdanov, M.S., 1986. Electrical Prospecting [in Russian]. Nedra, Moscow.

Editorial responsibility: M.I. Epov